Adsorption of Benzene Vapor onto Activated Biomass from Cashew Nut Shell: Batch and Column Study

Article · July 2012

DOI: 10.2174/2211334711205020116

4 authors, including:

Suresh Sundaramurthy
Maulana Azad National Institute of Technology, Bhopal, India & CUNY, New York, USA
142 PUBLICATIONS **936** CITATIONS

SEE PROFILE

Adsorption of Benzene Vapor onto Activated Biomass from Cashew Nut Shell: Batch and Column Study

S. Suresh[1,*], G. Vijayalakshmi[2], B. Rajmohan[2] and V. Subbaramaiah[3]

[1]*Department of Chemical Engineering, Maulana Azad National Institute of Technology Bhopal, Bhopal-462 051, India;* [2]*Department of Chemical Engineering, National Institute of Technology Karnataka, Surathkal, Srinivasnagar PO, Surathkal, Mangalore 575 025, India;* [3]*Department of Chemical Engineering, Indian Institute of Technology Roorkee, Roorkee- 247 667, Uttarakhand, India*

Received: January 03, 2012 Revised: June 16, 2012 Accepted: June 17, 2012

Abstract: The preparation of chemically modified activated cashew nut shell (ACNSB) of different impregnation ratios and their effects in adsorption of benzene vapor were studied. Effects of chemical pre-impregnation using phosphoric acid at different ratios (1:1 and 2:1) were investigated in order to patent. Physico-chemical characterization including surface area, scanning electron microscopy, energy dispersive X-ray spectroscopy, High-resolution Transmission Electron Microscopy and Fourier transform infrared spectroscopy of the ACNSB before and after benzene adsorption have been done to understand the adsorption mechanism. Optimum conditions for benzene removal were found to be, adsorbent dose m=10 g/l of solution and time (t) 120 min for the C_0 range of 300–500 mg/l. Adsorption of benzene followed pseudo-second-order kinetics. Langmuir and R–P isotherms were found to best represented data for benzene adsorption onto ACSNB. In ACNSB column experiments, it can be concluded that concentration of benzene increases with the longer breakthrough time and hence higher adsorption capacity. ACSNB are many advantages includes simple and fast, organic solvent recovery, economical, energy savings, environmentally safe aspect and minimize the waste management problem.

Keywords: Adsorption, Benzene, cashew nut shell, ACNSB, phosphoric acid.

INTRODUCTION

Industrial activities that emit large quantities of flues gases containing both organic and inorganic gases, especially volatile organic compounds (VOCs) are the major contributors of acid rain and generation of precursors of photochemical oxidants and depletion of stratospheric ozone layer. The major sources of these VOCs are emissions from petroleum industries, thermal power plants, paint industries, steel manufacturing industries etc. Volatile organic gases like benzene are emitted from a wide variety of miscellaneous sources like oil and natural gas wellheads, glycol dehydrators, petroleum refining, gasoline marketing, wastewater treatment, landfills, pulp and paper mills, and other mobile sources. The 1990 Clean Air Act Amendments enlisted around 188 hazardous air pollutants, among which VOCs are also listed. Thus VOCs are dangerous to the environment and carcinogenic to human life, even at very low concentrations like benzene is 5μg/m^3 [1]. The preparation of activated biomass from agricultural wastes which is valuable adsorbents, such as coconut shells [2], bagasse [3], coir pith [4], and agricultural residues from rice husk [5], peanuts [6], sawdust [7], and canes from some easy-growing wood species [8].

Ali and Gupta [9] described salient features of adsorption and details experimental methodologies for the development and characterization of low-cost adsorbents, water treatment and recycling including batch processes and column operations. The utilization of all such materials as low-cost adsorbents for the treatment of wastewater may make them of some value. An effort has been made to given a brief idea of an approach to wastewater treatment, particularly discussing and highlighting in brief the low-cost alternative adsorbents with a view to utilizing these low-cost materials [10]. for example: Gupta *et al.* [11] investigated adsorption methods for color removal from wastewater using waste materials activated carbon and activated rice husk. Carbon slurry, produced in fuel-oil-based industrial generators was converted into an effective and efficient adsorbent for the removal of endosulfan and methoxychlor from aqueous solution [12]; two reactive dyes from synthetic textile wastewater [13, 14]; fluoride from aqueous solution [15]; and it was observed that waste carbon slurry was effective adsorbent in terms of performance and cost especially.

Most of the activated biomass is produced by a two-stage process carbonization followed by activation. The first step is to enrich the carbon content and to create an initial porosity and the activation process helps in enhancing the pore structure. Girgis *et al.* [16] reported phosphoric acid inflicted physical and chemical modifications on the botanical structure by penetration, particle swelling, and partial dissolution of the biomass, bond cleavage and reformation of new of new polymeric structures resistant to thermal decomposition.

VOCs abatement can be done using thermal oxidizers, selective catalytic reduction scrubbers, biofiltration, absorption, adsorption, photo catalytic oxidation, and plasma tech-

*Address correspondence to this author at the Department of Chemical Engineering, Maulana Azad National Institute of Technology Bhopal, Bhopal-462 051, India; Tel: +918989005393;
E-mail: sureshpecchem@gmail.com

1874-4788/12 $100.00+.00

nique [17]. However all these processes have some economical constrains. An eco-friendly and economically viable technology are much desirable in the recent days. Many researchers have studied the elimination and recovery of VOCs using various activated carbons [18]. Puri *et al.* [19] studied on adsorption of benzene on sugar charcoal. Zhang *et al.* [20] studied on NO adsorption on activated carbons in the presence of oxygen. The presence of oxygen significantly enhances both physical and chemical adsorption. Bhatia *et al.* [21] observed experimental variables in the adsorption studies were gas flow rate, VOC concentration and the type of VOC. They found that removal efficiencies of greater than 95% are achievable for a variety of solvents. Oxidation method simply to destruct the organic solvents into harmless materials such as CO_2 and H_2O, but it is impossible to reuse the VOC, expensive and energy exhausting [21]. Popescu *et al.* [22] studied behavior of adsorption and desorption of toluene, butyl acetate, and butanol on activated carbons. Harikrishnan *et al.* [23] investigated adsorption characteristics of ethyl benzene according to pressure and temperature, and experimental results using activated carbon in the benzene recovery process [17]. Kim *et al.* [24] studied the adsorption characteristics of benzene onto activated carbon fixed bed reactor, and Kim *et al.* [25] studied adsorption of three major solvent vapors such as n-hexane, toluene, and MEK on two pelletized commercial activated carbons. Yun *et al.* [26] studied dynamic behavior of non-ideal gas mixtures in an isothermal fixed-bed absorber. They found that adsorption was more efficiency and economical method. Activated biomass adsorption has been used as most versatile adsorbent for quick and effective removal of VOCs and NO from the effluent streams [20].

CNSL is useful for insecticidal, fungicidal, anti-termite and medicinal applications [27-32]. As an agro-byproduct, it has the advantages of low cost and renewable supply [33]. Resins derived from CNSL are widely employed in the fields of friction materials, automobiles, surface coatings, adhesives, laminates, rubber compounding, and several miscellaneous applications [34]. The most attractive reasons for use of CNSL in industry are its low cost, abundant availability and chemically reactive nature. In industrial practice, drying oils are most frequently used to form resins due to their high ability for autoxidation, peroxide formation, and subsequent radical polymerization, as currently applied in paint and coating formulations [35, 36].

The interest in the development of cost effective methods for the removal of benzene vapor from effluent stream has greatly increased and using different activated biomass from the agricultural wastes.

The present investigation reports the results of removal of benzene vapor from by adsorption onto activated cashew nut shell biomass (ACNSB) prepared from low cost cashew nut shell (CNS) by different pre-impregnation ratios (1:1 and 2:1) with H_3PO_4 solutions. ACNSB has been characterized for its physico-chemical characteristics such as, surface area, and surface functional groups. Scanning electron microscopy (SEM), energy dispersive X-ray spectroscopies (EDX), Fourier transform infrared (FTIR) spectroscopy have been used to understand the mechanism of benzene adsorption onto ACNSB. Single solute gas phase adsorption isotherms and kinetics were conducted in this study to evaluate the effectiveness of a simple constant volume method. To analyze the breakthrough curves for the adsorption of benzene on the adsorbent in a packed column by varying operating parameters like inlet concentrations of benzene and adsorbent (1:1 and 2:1) impregnation ratio.

MATERIALS AND METHODS

Materials

An exhausted cashew nut shell–waste (CNSW) cake, obtained from Achel Industries in baikampady industrial Estate, Mangalore, India. Liquid benzene of 99.9% grade was obtained from REAKEM Chemical Co., Ltd. India.

Preparation of Activated Cashew Nut Shell Biomass (ACSNB)

The application of heat to impregnated material further accelerates the thermal degradation and volatilization process and leads to development of pores, increase of surface area and the subsequent mass loss [37]. The CNSW was washed with tap water and finally with distilled water until washed water becomes colorless. After dried materials were subjected for chemical activation of the precursor was done with H_3PO_4. Phosphoric acid was dissolve in water for reaching 40% concentration in weight and then impregnated into the shells with a certain impregnation ratio (defined by the weight ratio of H_3PO_4 to CNSW) i.e. 1:1 and 2:1. After then, slurry was kept in incubator shaker at 110^0C for 12 h. The resulted chemical-loaded samples were placed in a stainless-steel tubular reactor and heated (5^0C/min) to the final carbonization temperature under a nitrogen flow rate of 150 ml/min. Samples were kept at the final temperature (carbonization temperature) for carbonization times of 20 to 40 min before cooling down under nitrogen. Nitrogen entering in the reactor was first preheated to 250-300^0C in a pre-heater. The products after activation were thoroughly washed with water, followed by 0.5 M hydrochloric acid, then hot and cold distilled water to remove the residual H_3PO_4, residual organics and mineral matter until the pH value of the washed solution was between 6 and 7. Finally the sample was then dried at 105 °C and stored in desiccators for subsequent analyses and uses. Overall flow diagram is shown in (Fig. **1**). The proximate, ultimate, and component analyses of ACSNB were shown in Table **1**. This agricultural waste is considered as a good feasible idea for conversion to activated carbon because of its relatively high carbon content and low ash.

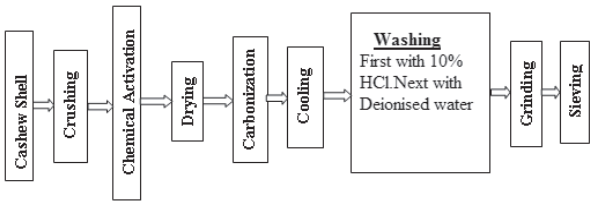

Fig. (1). Flow diagram for preparation of the activated CNSB.

Table 1. Physico-chemical Characteristics of the Cashew Nut Shell Waste and Activated CNSB

Composition (%) / Parameter	Cashew Nut Shell	After Treated with H_3PO_4	
		Ratio 1:1	Ratio 2:1
BET surface area (m^2/g)	771	886	903
Average pore diameter (nm)	2.80	2.92	3.02
Average pore volume (cm^3/g)	0.312	0.450	0.492
Moisture	9.03	8.95	6.93
Ash	0.61	0.42	0.435
Volatile matter	36.23	25.92	33.02
Fixed carbon	51.11	59.14	56.29
Iodine number	612.3	701.0	810.4
Carbon	81.01	85.49	87.46
Oxygen	10.51	10.77	11.69
Silica	0.17	0.24	1.73
Phosphorus	3.50	5.75	6.34
Aluminum	0.21	0.51	0.64

Characterization of Activated Biomass

To understand the morphology of the ACSNB, a scanning electron microscope (SEM) (QUANTA, Model 200 FEG, Netherland) and High-resolution Transmission Electron Microscopy (TEM) was carried out with an FEI Technai G^2 F20 microscope at 200 kV were used. The samples were air dried before using the TEM to characterise the size and morphology of the dried particles. Samples were first gold coated using a sputter coater, (Edwards S150). Gold sputtering provides conductivity to the samples, and then SEM and simultaneously elementary analysis was done using an EDAX spectrometry. For TEM observation, the samples were prepared in methanol at 100 µg/mL concentration and dispersed in an ultrasonicator for ten minutes. The samples for TEM analysis were obtained by placing a drop of the colloidal dispersion containing the CNSB or ACNSB onto the carbon-coated copper grid. They were dried at room temperature and then examined using the TEM without any further modification. The particle sizes in morphology were measured using a scale bar in micrographs.

Textural characteristic of the ACSNB was determined by nitrogen adsorption at 77.15 K using automatic pulse chemisorption system (Micromeritics Chemisorb 2720). The Brunauer–Emmett–Teller (BET) surface area [38] and monolayer pore volume of the ACSNB, before and after adsorption of benzene, were determined using software available with the instrument. FTIR spectrometer (Thermo Nicolet, NEXUS, USA) was employed to determine the presence of functional groups in the ACSNB, before and after the adsorption of benzene at room temperature. Pellet (pressed-disk) technique has been used for this purpose, and the spectral range was kept from 4000 to 400 cm^{-1}. The iodine number is defined in terms of the ml of iodine adsorbed by 1 g of activated biomass when the iodine equilibrium concentration is 0.01 M [39]. It was the measure of the micro pore content of the activated biomass by adsorption of iodine from sample. The procedure of the iodine number determination is as follows: two dry samples of activated biomass i.e. 1:1 and 2:1 impregnation ratio were weighed out into two 250-ml conical flasks (sample weight ranged between 300 and 600 mg). 10ml of 5% (in weight) hydrochloric acid solution were added to each flask and then mixed until the biomass became wet. The mixtures were then boiled for 30 sec and finally cooled. 100 ml of 0.05 M standard iodine solutions were added to each flask. The contents were vigorously shaken for 30 sec and then immediately filtered. A 50 ml aliquot of each filtrate was titrated by standardized 0.1 M sodium thiosulfate solution. The results are shown in Table **1**.

Analytical Techniques

Influent and effluent benzene gas concentrations were determined using gas chromatograph (NETEL India Ltd., Mumbai, India) equipped with a capillary column (25 m×0.32 mm) and a flame ionization detector connected with a computing integrator [40]. The temperatures of injector, oven and detector were 170, 150 and 270 °C, respectively. The carrier gas was nitrogen. 0.5 ml of air samples were injected into the FID gas chromatograph with a 1.0 ml gas-tight syringe and the benzene concentration was quantified by comparison with standards. Vapor phase pollutant standard curves were obtained by injecting known volumes of benzene, using a 10 µL liquid-tight syringe, into a sealed calibrated glass collector (200 ml), equipped with teflon-faced rubber septa according to the methods described by Lodge [41]. The pollutant was allowed to evaporate completely at room temperature for 12 h within the collector.

Then, gas samples were withdrawn from the bottles with a 1.0 ml gas-tight syringe and 0.5 ml was subjected to gas chromatograph analysis.

Batch Study

To study the constant volume single phase adsorption for removal of benzene were carried out in Gas Sampling collector. Adsorption experiments were conducted in batch mode using the experimental setup as shown in (Fig. **2**). The adsorption isotherms and kinetics that relate the concentration of benzene in the adsorbed state versus its gas phase concentrations were determined. Each point was obtained by using a 'Gas Sampling collector', each collector has two port, One was used for pumping air/gas and the other port, which has a threaded cap with septa, issued to insert the adsorbent and later for sampling purposes. Different masses of the adsorbents were carefully weighed and placed inside each collector through the port provided. Masses of the ACSNB ranged from 5, 10, 15, 20 and 25g per collector. ACSNB was prepared in the particle size of 2 to 4 mm [42]. Adsorption experiments are conducted at room temperature, and the glass collecter is a borosilicate glass of 50 mm inside diameter and height 150 mm. Air from an air pump is first fed to the heater to the aspirating bottle, benzene vapors are produced by vaporizing liquid benzene with hot air from a compressor through an air heater at different flow rates. An air rotameter of range 0 to 10 lpm is used to measure and regulate the flow rate of air from the compressor and the vapors fed into the gas collector and it pass through the ACSNB, after 5 minutes closed the both of the gas collector to ensure that it was accurately filled with the benzene in the collector. Through initial testing, it was found that 2.3 h were enough for attaining equilibrium. Gas samples were taken and analyzed every 5 min to determine the equilibrium gas phase concentrations of benzene. The collectors were turned over every 5 minutes ensure proper contact of the adsorbent with the benzene. In this study, the percentage benzene loss was independent on the initial concentration of benzene and the type of ACSNB The batch adsorption study was done for 300 400 and 500 mg/l of benzene concentration of 5, 10, 15, 20, 25 g masses of ACSNB for different ratio (1:1, 2:1).

The Benzene removal from the sample was calculated as:

$$\% \text{ Benzene removal} = 100(C_0 - C_t)/C_0 \quad (1)$$

and the adsorptive uptake of benzene by ACSNB (mg/l), was calculated as

$$q_t = (C_0 - C_t)V/w \quad (2)$$

Where, C_o is the initial benzene concentration (mg/l), C_t is the benzene concentration (mg/l) at any time *t*; V is the volume of the solution (l) and w is the mass of the ACSNB (g).

Column Study

Experimental arrangement used for the dynamic packed column studies was same as used by in their study for adsorptive removal of acetone and toluene vapor using granular activated carbon [43]. ACSNB was prepared in the particle size of 2-4 mm, and was used as adsorbent. Adsorption experiments are conducted in continuous mode using the experimental setup as shown in (Fig. **2**). The experimental setup consists of a vapor generation unit and an ACSNB bed for adsorption. Adsorption experiments are conducted at room temperature, and the ACSNB bed column is a borosilicate glass of 5 cm inside diameter and height 20 cm. Air from an air pump was first fed to the heater to the aspirating bottle, vaporizing liquid benzene with hot air from a compressor through an air heater at different flow rates. An air rotameter of range 0 to 10 lpm was used to measure and regulate the flow rate of air from the compressor and the vapors fed into the bottom of the reactor to pass through the activated biomass bed in a counter and flowed out from the upside. The upside of the reactor is packed with ACSNB impregnated ratio (1:1and 2:1). Sampling points are provided at the inlet and outlet of the column for drawing the gaseous samples at regular intervals of time and analysis can be done with gas chromatograph (Hewlett-Packard Company).

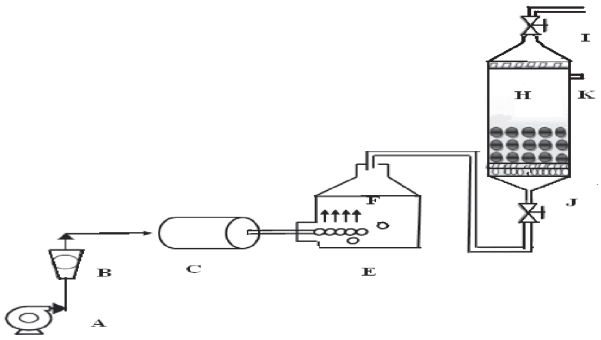

Fig. (2). Schematic diagram of the experimental set up.
A - Air supply, B- Rota meter, C - Air heater F- Air distributor E- Aspirating bottle containing liquid benzene, H- (Activated biomass), I, J - Sample ports K-Septum.

RESULTS AND DISCUSSIONS

Characterization of ACSNB

Detailed physico-chemical and textural characterization of the fresh and some of the characteristics of benzene loaded ACSNB is given in Table **1**. The BET surface area of Cashew nut shell and ACSNB (1:1 and 2:1) were found to be 771 m^2/g, 886 m^2/g and 903 m^2/g respectively. The moisture content of the ACSNB with chemical impregnation ratio 1:1 is found to be higher than the sample with chemical impregnation ratio 2:1. For ACSNB activated with H_3PO_4 the moisture content decreases with increase in the impregnation ratio. Both the samples are hygroscopic and hence absorb moisture. For phosphoric acid impregnated sample the moisture content decreases from 7.5 to 6.487 %. Ash content for activation with H_3PO_4 for 1:1 impregnation ratio ash content is lower because H_3PO_4 decomposes while carbonizing, and hence doesn't remain in the ash. However some amount of phosphorus may remain as ash due to which ash content increases with increase in impregnation ratio. Volatility of samples activated with H_3PO_4 is more as it is strong acid and strong dehydrating agent, which weakens the cellulose bonds increasing the volatility of the sample (29.56% to 33.32%). The iodine number indicates developed pore volume.

However it can be seen that when the sample impregnated with H_3PO_4 (2:1) had iodine number of 810.4; H_3PO_4 (1:1) had iodine number 612.30. As the impregnation ratio increases pore development increases and hence the iodine value. It can also be noted that the iodine number of activated samples impregnated with activating agent falls well within the desirable region of 600 - 1100. The iodine number obtained shows that the activated carbon produced by impregnating cashew nut shell has a good competence with commercially available activated carbon. SEM images of the sample impregnated with H_3PO_4 (1:1 and 2:1) were shown in the (Fig. (**3**) **a, b & c**)). There were very little pores like cylindrical pores and slit-shaped pores formed on the surface of the sample with 1:1 impregnated ratio. However, sample with 2:1 impregnated ratio has many large pores like a honeycomb shape were developed on the surface of the ACSNB and a smooth melt surface appeared, interspersed with generally large pores was due to some of the volatiles being evolved as shown in (Fig. **3a**). As it can be seen from (Figs. **3b & 3c**) the reduction of the surface area, partial blocking of pores was observed after adsorption of benzene [44]. There are two distinct types of patterns were observed that the change in the color and formation of cavities on the surface indicates the adsorption of benzene vapor in the form of thin layer as mentioned by Tansel and Nagarajan [45] for phenolphthalein adsorption on granular activated carbon. Similar pattern can be observed for both adsorbents. EDX was conducted to study the distribution of elements before and after adsorption of benzene onto ACSNB (Table **1**). Fresh-ACSNB was found to contain 81.01% carbon, 10.51% oxygen, and rest others. Impregnated ratio 1:1- and 2:1-loaded ACSNB were found to contain 85.5% and 87.5% carbon, 10.77% and 11.69% oxygen, respectively, and rest others. Thus, the amount of carbon increased in ACSNB after the loading of impregnated ratio 1:1- and 2:1 onto ACSNB.The typical microstructure of before and after activated cashew nut shell biomass by TEM studies (Fig. **4a-b**). TEM photographs show that the average particle size was 25 nm, and the corresponding electron diffraction pattern showed only diffused signals, as expected for amorphous materials.

FTIR spectroscopy is an important analytical technique that detects the vibration characteristics of chemical functional groups present on adsorbent surfaces. The FTIR spectrum obtained for both before and after adsorption of benzene are plotted and shown in the (Figs. **5a, b, c**. Fig **5a**) indicates that before adsorption of benzene onto fresh cashew net shell displayed the following bands. The functional groups present on the samples are observed to be phenols and alcohols, lactones typical acidic functional groups [46]. 1050- 1200 cm^{-1} C-OH stretching vibration in alcohols (1200–1257 cm^{-1}), 3593-3643 cm^{-1} free O-H stretches (assignment range 3635–3610 cm^{-1}), 2000 -1700 cm^{-1} C=C

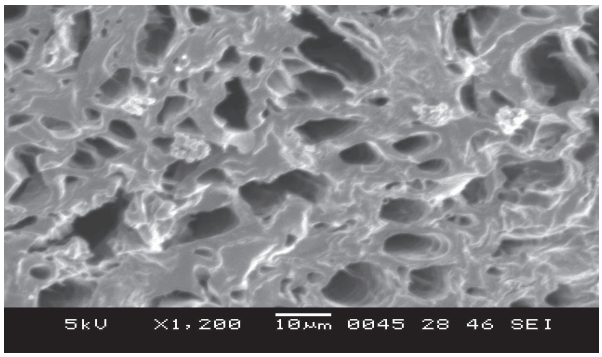

(a) Fresh cashew nut shell waste

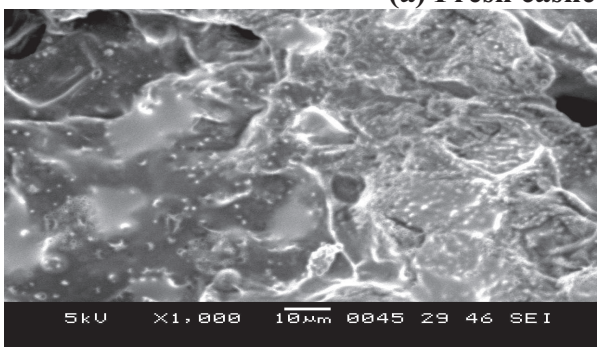

(b) Sample with chemical impregnation ratio 1:1

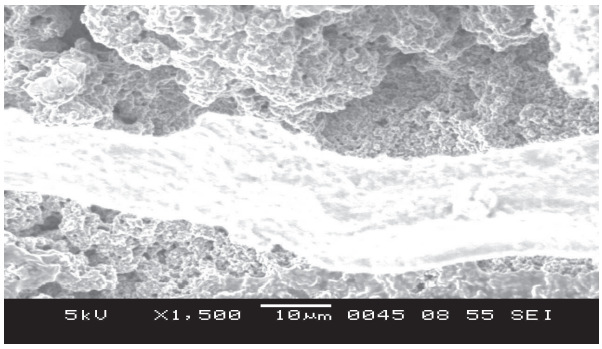

(c) Sample with chemical impregnation ratio 2:1

Fig. (3). SEM of before and after loaded activated cashew nut shell biomass.

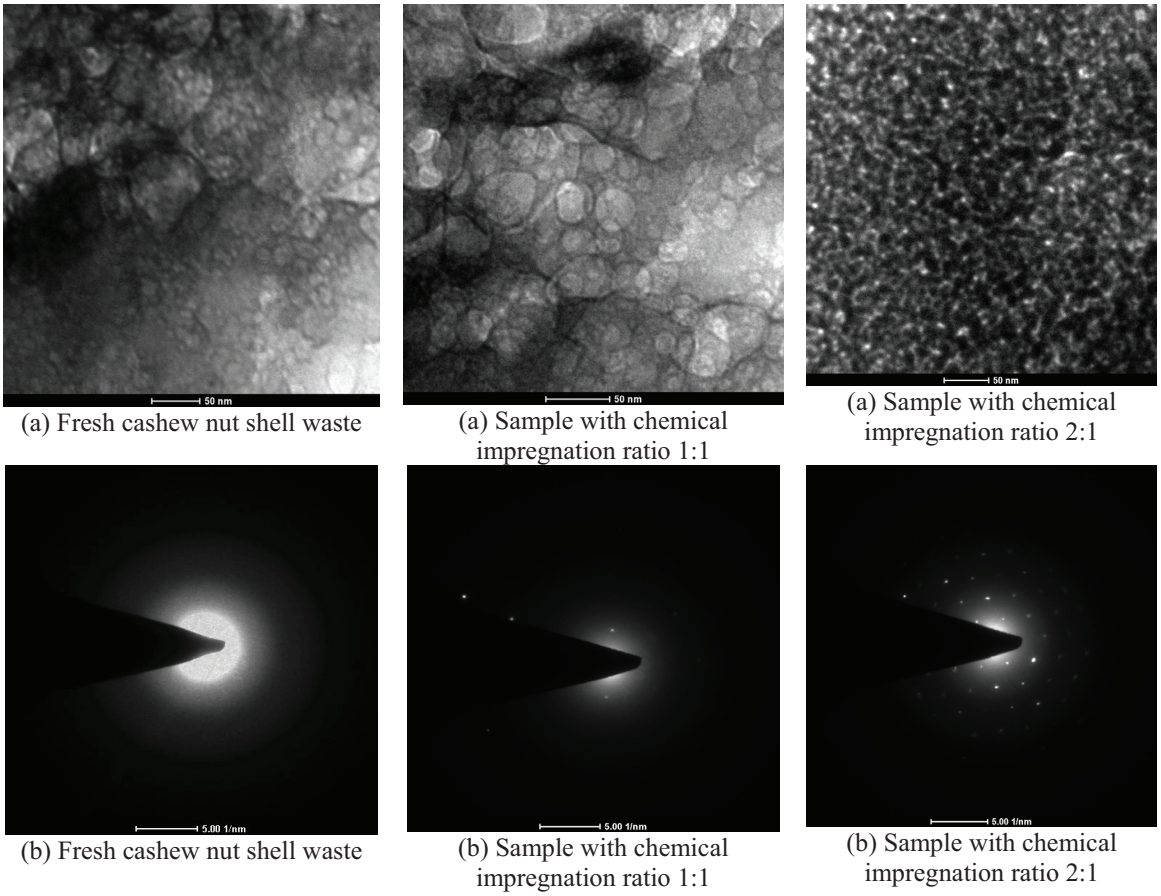

(a) Fresh cashew nut shell waste

(a) Sample with chemical impregnation ratio 1:1

(a) Sample with chemical impregnation ratio 2:1

(b) Fresh cashew nut shell waste

(b) Sample with chemical impregnation ratio 1:1

(b) Sample with chemical impregnation ratio 2:1

Fig. (4). (**a**) Representative TEM image of Fresh and activated cashew nut shell biomass (scale bar represents 50 nm) and (**b**) the corresponding diffraction pattern.

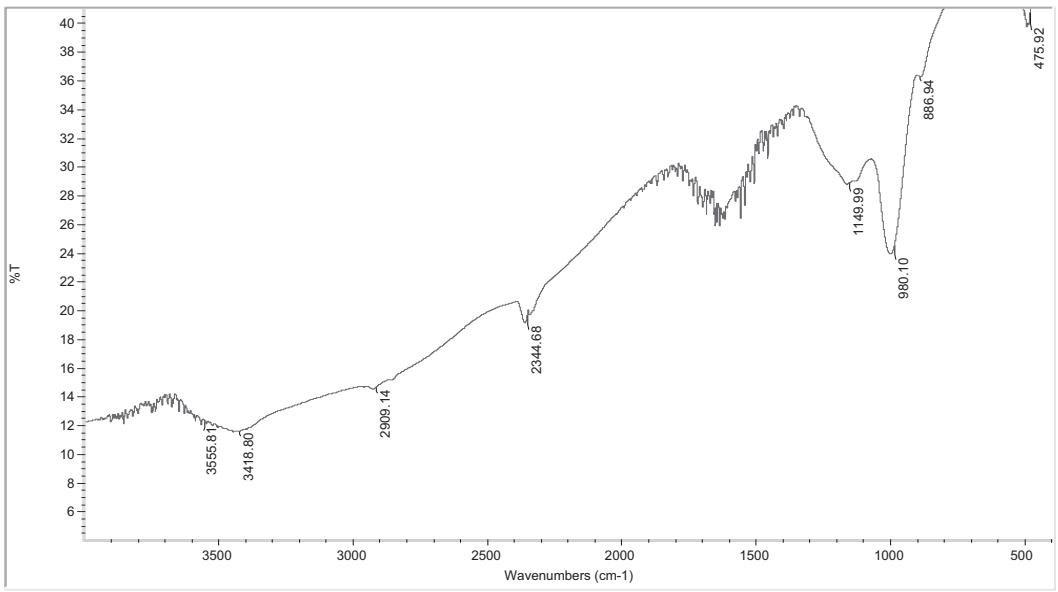

(a) Fresh cashew nut shell waste

(Fig. 5) contd….

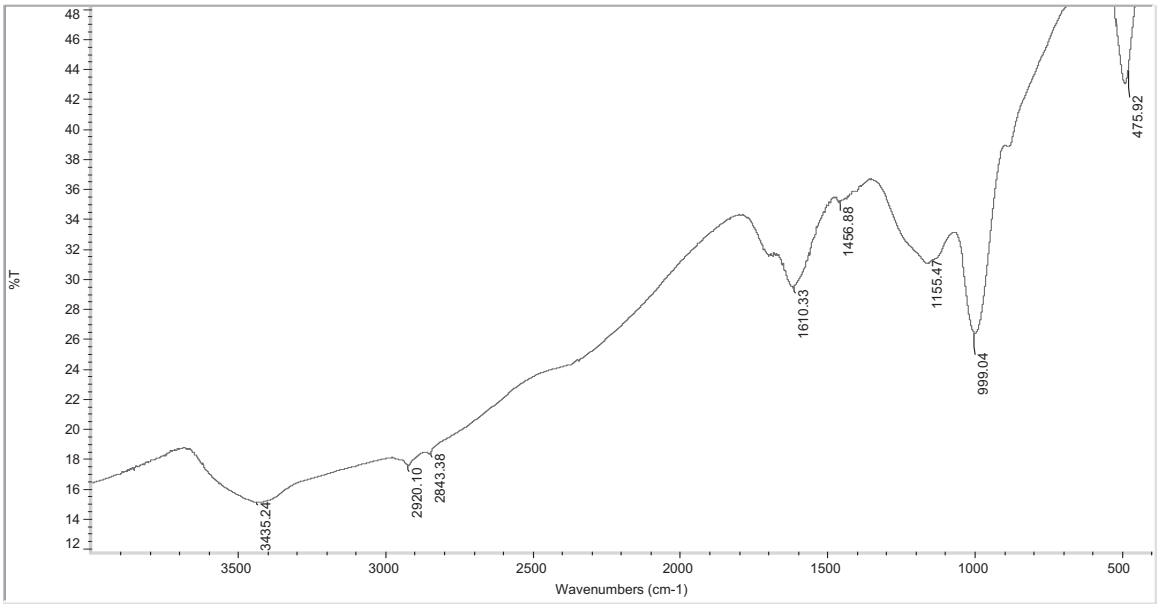

(b) Sample with chemical impregnation ratio 1:1

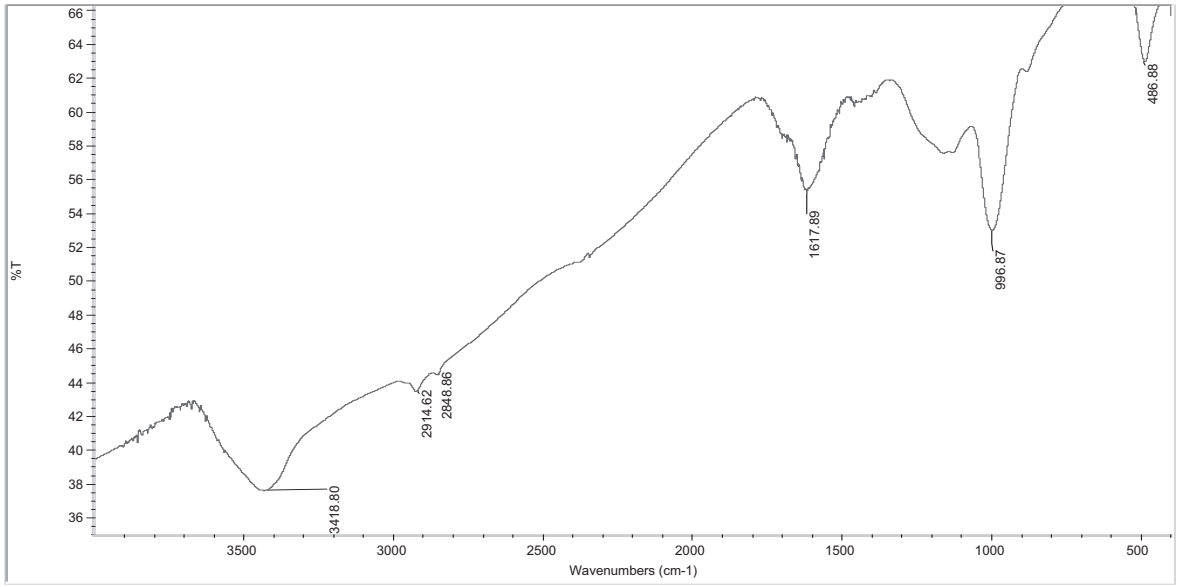

(c) Sample with chemical impregnation ratio 2:1

Fig. (5). FTIR of Fresh, loaded activated cashew nut shell biomass.

stretching vibration in aromatic rings. After adsorption of benzene (Fig. **5b, c**) displays the following bands. The surface organic functional groups present of the samples after adsorption of the benzene vapors are phenols, alcohols and amine groups formed on the sample surface. 1050- 1200 cm^{-1}, C-OH stretching vibration in alcohols (1200-1257 cm^{-1}), 3593-3643 cm^{-1}, free O-H stretches [assignment range is 3635-3610 cm^{-1}), 3400-3380, 3345-3325 cm^{-1}, NH stretching, primary amines, 3360 - 3310 cm^{-1}, NH stretching, secondary amines, 1650-1590 cm^{-1}, NH deformations, primary mines, 1650-1550 cm^{-1}, NH deformations, secondary amines, 1080-1040 cm^{-1}, C-N Stretching, primary amine and 1180-1140 cm^{-1}, pyrones, C-N stretching, secondary amines. The formation of stronger peaks for pyrone type structures, ether, carbonyl groups employed a basic character of ACSNB. In the Benzene-ACSNB spectra, only small band shifts are observed such as that for OH. These results suggest that the interaction of benzene to ACSNB occurred through hydrogen bond.

Effect of Adsorbent Dosage

The effectiveness of adsorbent dose on adsorption of benzene vapor by cashew nut shell waste pre-impregnated (1:1 and 2:1) with H_3PO_4 using simple constant volume method, is examined at operating parameters like room temperature 30 ^{0}C particle size of 2 to 5 mm, 200 ml volume of 300, 400 and 500 mg/l benzene concentration the adsorbent dose from 5 to 25 g and contact time of 150 minutes for both adsorbents (1:1 and 2:1). From the (Figs. **6,7** and **8**) shown that by increasing the adsorbent dose from 5 to 15 g the concentration decreases appreciably and for the 20 and 25 g of adsorbent dose the decrease in the concentration was same. From (Figs. **6, 7** and **8**) by increasing the adsorbent dose the percent removal of benzene increases but the percent removal was almost same for 20 and 25 g of adsorbent dose. Hence it is the optimum adsorbent dose for adsorbate concentrations of two adsorbents (1:1 and 2:1 impregnation ratio). Similar observation was also made by determination of the gas phase adsorption isotherms in the simple constant volume method. For 100ml of benzene having concentration range from 300 to 500 mg/l with 5 to 25 g of adsorbent the equilibrium was attained at 120 mins. Adsorption of benzene was measured at given contact periods for three different concentrations of 5, 10, 20, 15 and 25 g adsorbents for the both impregnation ratios. From the experimental data it can be observed that, the rate of adsorption starts decreasing remarkably although the sorption capacity for benzene concentration increases considerably. For both adsorbents the percentage removal efficiency of benzene are found to decrease with increase in the benzene concentration from (Figs. **6, 7** and **8**). In case of 1:1 impregnation ratio the benzene removal was less compared to 2:1 impregnation ratio. This behavior is due to the development of pores on the surface of adsorbent, organic functional groups and pores volumes were higher in case of 2:1 impregnation ratio and the uptake of benzene was high, hence rate of adsorption increases compare to the 1:1 impregnation ratio.

Effect of Contact Time

The effect of contact time on the removal of benzene by the ACSNB at C_0= 300, 400 and 500 mg/l for m=10 g/l, room temperature 30 ^{0}C, particle size 2 to 5 showed rapid adsorption of benzene in the first 15 min and, thereafter, the adsorption rate decreased gradually and the adsorption reached equilibrium in about 120 min as shown in (Fig. **5**). An increase in contact time up to 5h showed that the benzene adsorbed increased by only about 0.8% over that obtained at 120 min contact time. The gradual and steady decrease in benzene concentration was observed upto 150 minutes contact time (figures are not shown) indicates that beyond 120 min adsorption trend was found to remain constant for both impregnation ratio (1:1 and 2:1). Aggregation of benzene molecules with the increase in contact time makes it almost impossible for the benzene molecules to diffuse deeper into the adsorbent structure at the highest energy sites. This aggregation negates the influence of contact time as the mesopores get filled up and start offering resistance to diffusion of aggregated dye molecules in the adsorbents [47]. This is the reason why an insignificant enhancement in adsorption is effected in 5 h as compared to that in 120 min. Since the difference in the adsorption values at 120 min and at 5 h was very small, after 120 min contact, a steady-state approximation was assumed and a quasi-equilibrium situation was accepted. Further experiments were conducted for 120 min contact time only. Similar observation was also made by methyethylketone and benzene adsorption onto activated carbon fiber beds [48].

Effect of Initial Concentration

The effect of initial concentration on adsorption of benzene was determined by simple constant volume experiments at operating parameters at room temperature 30 ^{0}C, particle size of 2 to 5 mm, 100 ml volume of 300 to 500 mg/l concentrates of benzene and adsorbent dose of 5 to 25 g. For 200ml of adsorbate solution having concentration range from 300,400 and 500 mg/l with 5 to 25 g of adsorbent the equilibrium was attained at 120 mins. Adsorption of benzene was measured at given contact periods for three different concentrations of 5, 10, 15, 20 and 25 g adsorbents for the both impregnation ratios. These data reveals that as the initial concentration of benzene concentration decreases considerably with contact time and adsorbent dose. It was observed that concentration decreases with contact time, it reached to the constant beyond 120 min similar pattern was seen for both adsorbents (1:1 and 2:1 impregnation ratio) (figures are not shown). The inlet concentration of benzene decreases with adsorbent dose and percent removal increases. In case of 2:1 impregnation ratio the concentrations decreased was high, this behavior is due to formation of monolayer coverage of benzene vapor on adsorbent was high compare to 1:1 impregnation ratio because of development of pores and functional groups on the surface of adsorbent and hence up take of benzene increases). For a gas molecule has strong dipole moment, the adsorption of this gas molecule increases as the field of dipole interaction becomes significant reported by [49].

Adsorption Kinetic Study

In order to investigate the adsorption of benzene onto ACSNB, pseudo-first-order, pseudo-second-order, Bangham and intra-particle diffusion kinetic models were used.

The pseudo-first-order equation is given as [50].

$$q_t = q_e\left[1-\exp\left(-k_f t\right)\right] \tag{3}$$

Where, q_e = amount of the adsorbate adsorbed on the adsorbent under equilibrium condition and k_f is the pseudo-first-order rate constant.

The pseudo-second-order model is represented as [47, 51]:

$$q_t = \frac{tk_S q_e^2}{1+tk_S q_e} \tag{4}$$

The initial adsorption rate, h (mg/g min), at t→0 is defined as

$$h = k_S q_e^2 \tag{5}$$

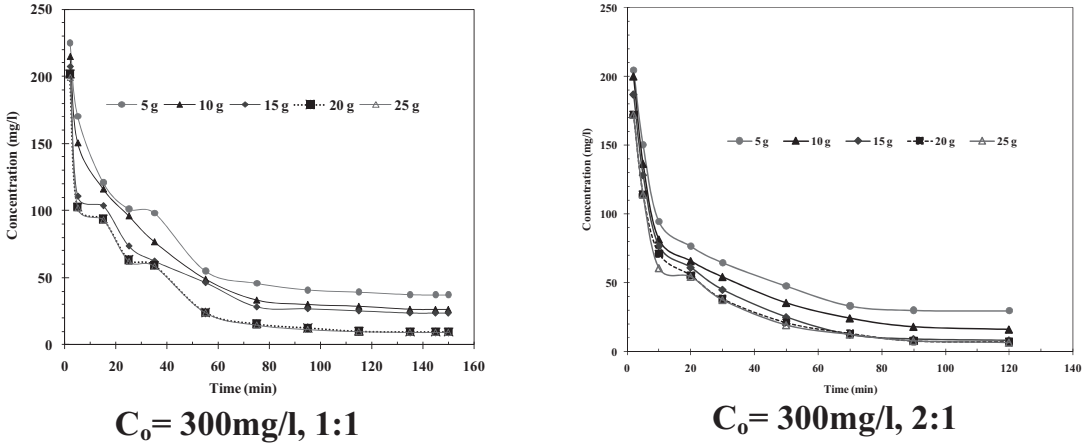

Fig. (6). Effect of adsorbent dose on benzene adsorption with time and C_o= 300mg/l. (**a**) 1:1 (**b**) 2:1 impregnation ratio.

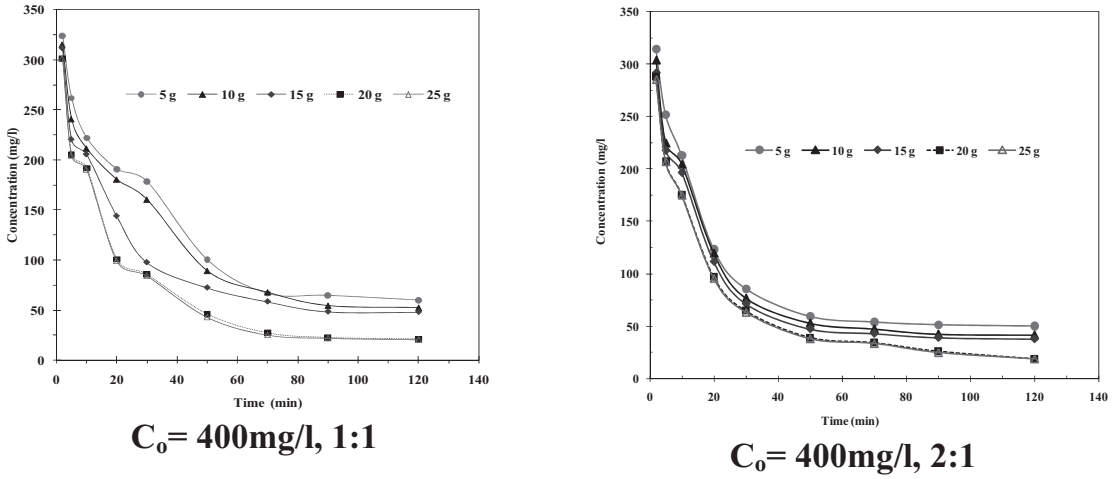

Fig. (7). Effect of adsorbent dose on benzene adsorption with time and C_o= 400mg/l. (**a**) 1:1 (**b**) 2:1 impregnation ratio.

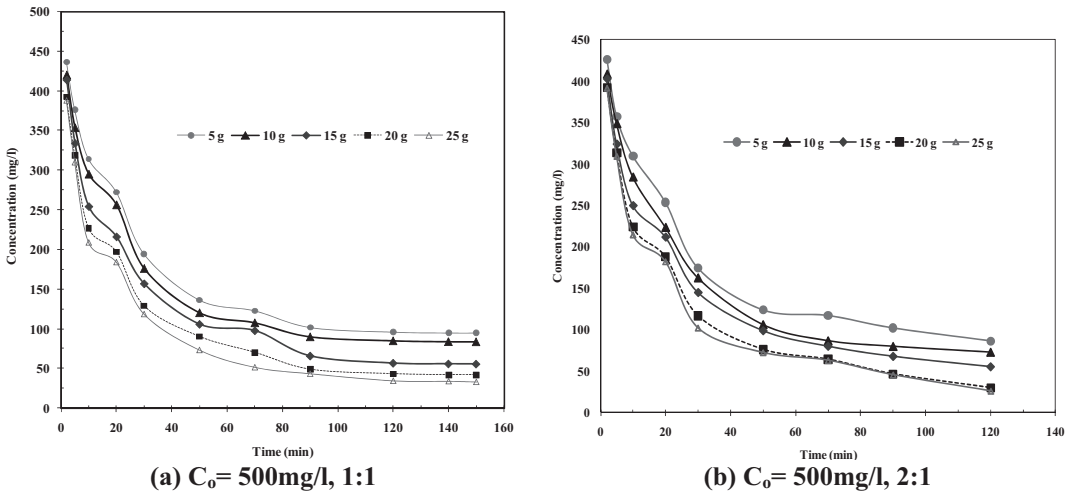

Fig. (8). Effect of adsorbent dose on benzene adsorption with time and C_o= 500mg/l. (**a**) 1:1 (**b**) 2:1 impregnation ratio.

Various error function were employed in this study to findout the most suitable kinetic and isotherm models to represent the experimental data. The error function is given in the Table **4**. The Marquardt's percent standard deviation (MPSD) error function [52], sum of square of errors (SSE), hybrid fractional error function (HYBRID) [53] and sum of the absolute errors (CH). In these equations, the subscript 'exp' and 'calc' represent the experimental and calculated values, n_m is the number of measurements, and n_p is the number of parameters in the model. MPSD error function was used to fit the kinetic models and similar error function has been used previously by a number of researchers in the field [47,54].

The q_e is obtained from the slope of t/q_t versus t (Fig. **9 a&b**) and h is obtained from the intercept. Since q_e is known from the slope, the k_S can be determined from the value of h. The best-fit values of h, q_e and k_S along with correlation coefficients for the pseudo-first-order and pseudo-second order models are shown in Table **2**. The $q_{e,exp}$ and the $q_{e,cal}$ values for the pseudo-first-order model and pseudo second-order models are also shown in Table **2**. The $q_{e,exp}$ and the $q_{e,cal}$ values from the pseudo-second-order kinetic model are very close to each other, and also, the calculated correlation coefficients, R^2 (both linear and non-linear) are also closer to unity for pseudo-second-order kinetics than that for the pseudo first-order kinetics. Therefore, the sorption can be more appropriately by pseudo-second-order kinetic model than the first-order kinetic model for the adsorption of benzene by ACSNB.

The possibility of intra-particle diffusion resistance affecting adsorption was explored by using the intraparticle diffusion model [55] where k_{id} is the intra-particle diffusion rate constant.

$$q_t = k_{id} t^{1/2} + I \quad (6)$$

Where, k_{id} is the intra-particle diffusion rate constant, and values of I give an idea about the thickness of the boundary layer.

In order to check whether surface diffusion controlled the adsorption process, the kinetic data were further analyzed using Boyd kinetic expression. In (Figs. **9 c&d**), a plot of q_t versus $t^{1/2}$ is presented for adsorption of benzene onto ACSNB. Values of I (Table **2**) give an idea about the thickness of the boundary layer, i.e., the larger the intercept, the greater is the boundary layer effect [47]. The deviation of

Table 2. Kinetic Parameters for the Removal of Benzene by ACNSB (t =120 min, C_o =300-500 mg/l, m =10 g/l, T=303 K)

Equations	1:1 Impregnated Ratio			2:1 Impregnated Ratio		
	300 mg/l	400 mg/l	500 mg/l	300 mg/l	400 mg/l	500 mg/l
Pseudo 1st order						
k_f (min^{-1})	12.16	28.88	6.923	11.03	23.66	7.690
$q_{e,cal}$ (mg g^{-1})	20.41	21.98	41.16	20.4090	21.9810	41.1633
$q_{e,\exp}$ (mg g^{-1})	27.37	34.78	41.61	28.3980	35.8660	42.7440
R^2 (non-linear)	0.7361	0.6623	0.9873	0.7771	0.6882	0.9928
MPSD	127.35	161.12	38.52	121.7645	169.6664	36.4195
Pseudo 2nd order						
k_s (g mg^{-1} min^{-1})	0.0077	0.0044	0.0022	0.0027	0.0014	0.0012
h (mg g^{-1} min^{-1})	6.1209	5.5807	4.3737	6.1209	5.5807	4.3737
$q_{e,cal}$ (mg g^{-1})	28.1781	35.8060	44.6317	28.1781	35.8060	44.6317
R^2 (non-linear)	0.9943	0.9818	0.9936	0.9969	0.9946	0.9968
MPSD	12.5829	26.2997	17.8917	22.5954	30.2334	20.3108
Weber Morris						
K_{id1} (mg g^{-1} $min^{-1/2}$)	0.2498	0.3824	0.5006	0.2128	0.2984	0.4896
I_1	0.2688	0.3488	4.8393	0.2688	0.3488	4.8393
R^2	0.9062	0.9727	0.9338	0.9062	0.9727	0.9338
K_{id2} (mg g^{-1} $min^{-1/2}$)	0.0321	0.0357	0.0980	0.0211	0.0217	0.0710
I_2	3.9694	7.8770	14.8920	3.9694	7.8770	14.8920
R^2	0.9115	0.8345	0.7596	0.9115	0.8345	0.7596

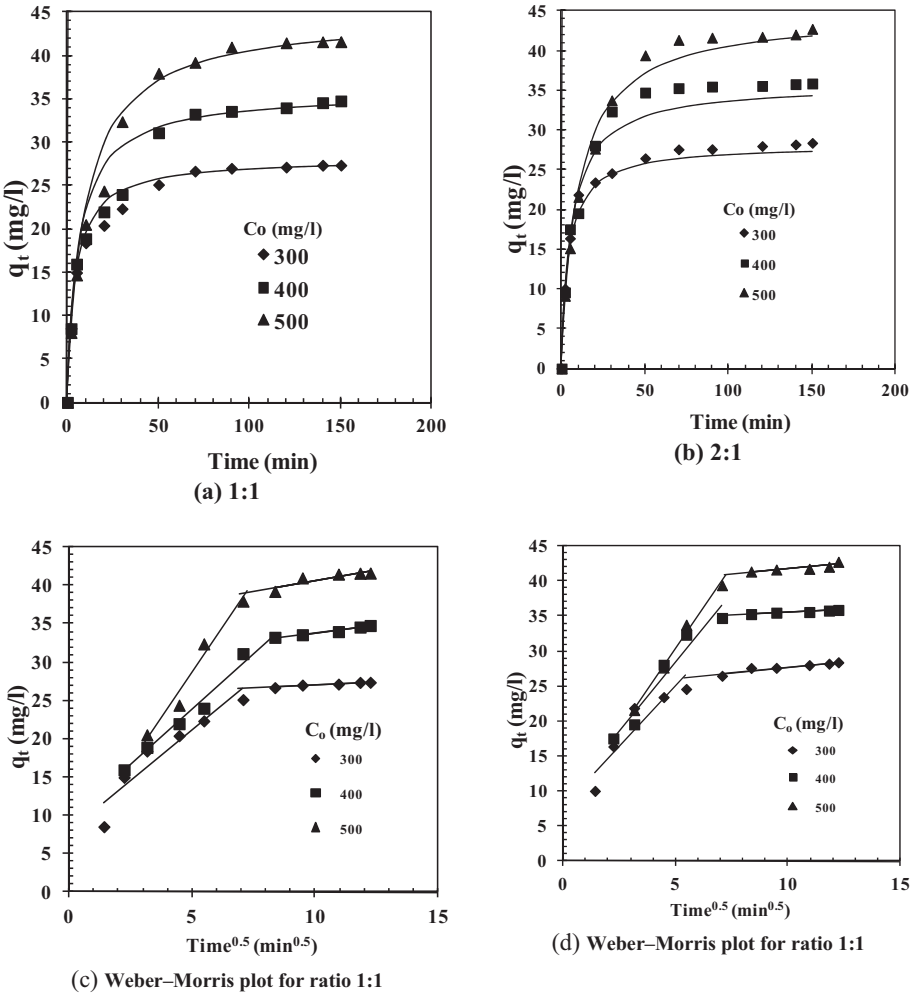

Fig. (9). Effect of contact time and initial concentration on the adsorption of benzene by ACNSB. (**a**) 1:1 impregnated ratio, (**b**) 2:1 impregnated ratio. Experimental data points given by the symbols and the lines predicted by the pseudo-second-order model. (**c**) Weber–Morris plot for ratio 1:1 and (**d**) Weber–Morris plot for ratio 2:1. t = 120 min, C_o=300-500 mg/l, m = 10 g/l.

straight lines from the origin (Figs. **9 c&d**) may be because of the difference between the rate of mass transfer in the initial and final stages of adsorption. Further, such deviation of straight lines from the origin indicates that the pore diffusion is not the sole rate-controlling step as shown earlier by Boyd kinetic expression. From (Figs. **9 c&d**), it may be seen that there are two separate regions-the initial portion is attributed to the bulk diffusion and the linear portion to intra-particle diffusion [47]. The values of $k_{id,1}$ and $k_{id,2}$ as obtained from the slopes of the two straight lines are listed in Table **2**.

Adsorption Equilibrium Study

To optimize the design of an adsorption system, it is important to establish the most appropriate correlation for the equilibrium curves. Various isotherm equations have been used to describe equilibrium characteristics of adsorption. Four isotherm equations namely Freundlich Freundlich [56], Langmuir Langmuir [57], Redlich-Peterson (R-P) [58] and Temkin [59] have been used in the present study to fitted experimental data for benzene adsorption onto ACSNB at 303 K with difference concentration (300-500 mg/l). Four errors function was used as a criterion in finding the best isotherm model to fit the experimental data. The Freundlich, Langmuir, R–P and Temkin isotherm constants were determined from the plots of q_e versus Ce (Figs. **10 & 11**) at 303 K using MS Excel 2007. The isotherm constants for all the isotherms studied, and the correlation coefficients, R^2 with the experimental data were listed in Table **3**. The correlation coefficients for the Langmuir isotherm are highest in comparison to the values obtained to Freundlich, R–P and Temkin isotherms. Therefore, the Langmuir isotherm is the best-fit isotherm for the adsorption of benzene onto ACSNB at 303 K. q_m is the monolayer saturation at equilibrium. The adsorption capacities of the two adsorbents (1:1 and 2:1 impregnated ratio) for three concentrations of benzene (300-500 mg/l). It is seen from (Fig. **11**) for impregnation ratio 2:1 has much higher adsorption capacity for benzene, while it provided comparatively lower adsorption capacity for 1:1 impregnation ratio.

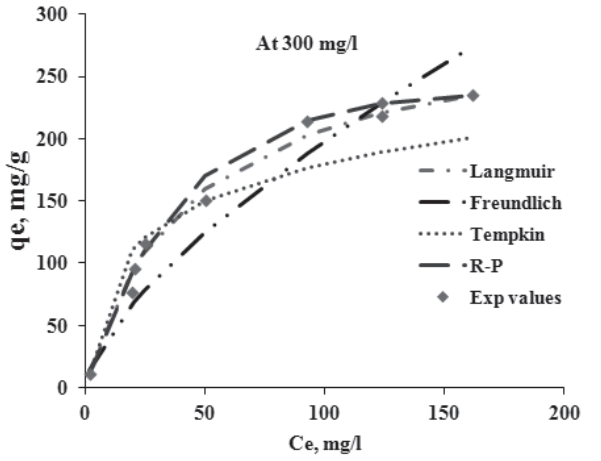

(a)

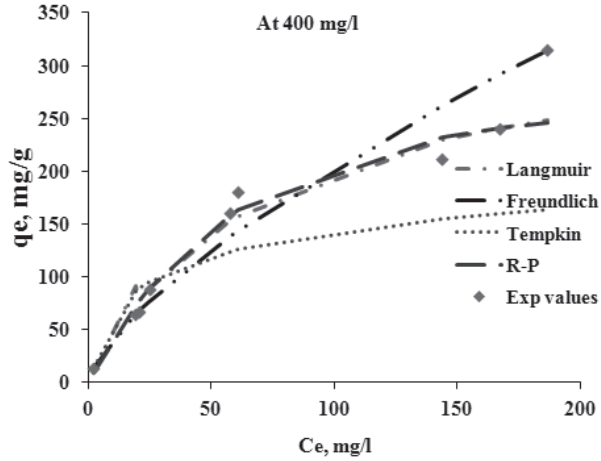

(b)

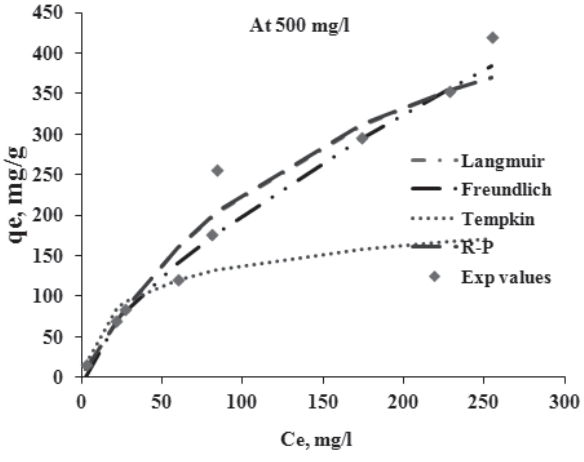

(c)

Fig. (10). Equilibrium adsorption isotherms at different temperature for benzene-ACNSB system (1:1 impregnation ratio), t=120 min, C_0=300-500 mg/l, m=10 g/l. Experimental best data points given by the symbols and the lines predicted by Langmuir, Freundlich, Tempkin and Redlich-Peterson equation. (**a**) 300 mg/l (**b**) 400 mg/l, (**c**) 500 mg/l.

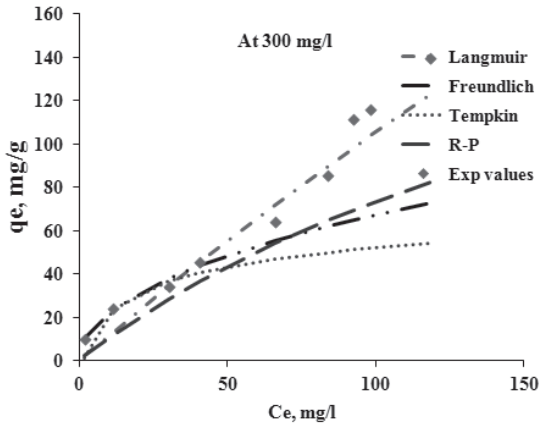

(a)

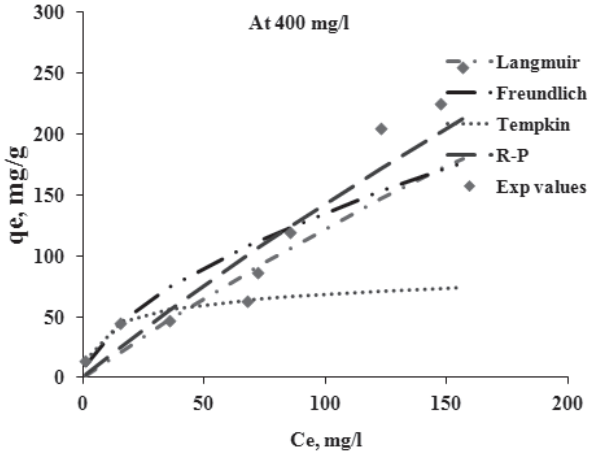

(b)

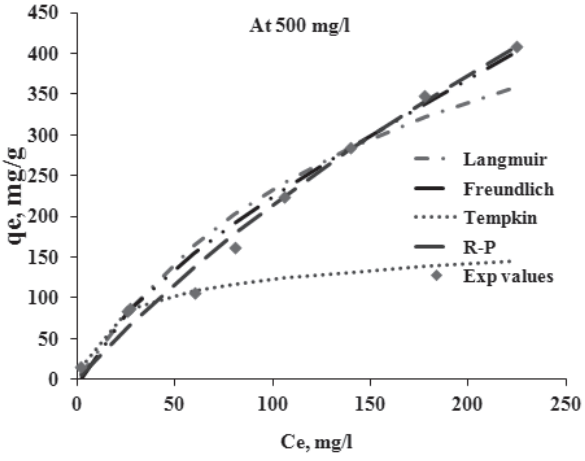

(c)

Fig. (11). Equilibrium adsorption isotherms at different temperature for benzene-ACNSB system (2:1 impregnation ratio), t=120 min, C_0=300-500 mg/l, m=10 g/l. Experimental best data points given by the symbols and the lines predicted by Langmuir, Freundlich, Tempkin and Redlich-Peterson equation. (**a**) 300 mg/l (**b**) 400 mg/l, (**c**) 500 mg/l.

Table 3. Isotherm Parameters for the Removal of Benzene by ACNSB (t=120 min, m=10 g/l, T=303 K). Benzene Adsorption onto ACNSB at Different Concentration

		1:1					2:1		
Isotherm	**Constants**	300 mg/l	400 mg/l	500 mg/l	**Isotherm**	**Constants**	300 mg/l	400 mg/l	500 mg/l
Langmuir	K_L (l/mg)	0.023	0.014	0.006	Langmuir	K_L (l/mg)	0.001	0.0012	0.006
	q_m (mg/g)	298.34	342.92	626.43		q_m (mg/g)	1095.26	1064.09	629.15
	R^2	0.995	0.967	0.977		R^2	0.983	0.961	0.973
Freundlich	1/n	0.671	0.699	0.696	Freundlich	1/n	0.476	0.589	0.724
	K_F ((mg /g) (mg/l) $^{1/n}$)	8.90	8.11	8.09		K_F ((mg /g) (mg/l) $^{1/n}$)	7.49	8.98	7.94
	R^2	0.968	0.966	0.978		R^2	0.943	0.924	0.988
Temkin	B	43.16	34.15	34.82	Temkin	B	13.00	12.54	27.41
	K_T (l/mg)	0.646	0.656	0.528		K_T (l/mg)	0.550	2.35	0.866
	R^2	0.969	0.923	0.899		R^2	0.841	0.751	0.848
Redlich-Peterson	Ar (l/mg)$^{1/\beta}$	0.005	0.004	0.005	Redlich-Peterson	Ar (l/mg)$^{1/\beta}$	0.006	0.006	0.013
	K_R (l/g)	5.58	4.28	3.52		K_R (l/g)	1.07	1.68	2.78
	β	1.26	1.190	1.034		β	0.960	0.712	0.685
	R^2	0.994	0.964	0.976		R^2	0.968	0.962	0.992

Freundlich: $q_e = K_F C_e^{1/n}$; **Langmuir:** $q_e = \frac{q_m K_L C_e}{1 + K_L C_e}$;

Temkin: $q_e = B_T \ln(C_e K_T)$; **R-P:** $q_e = \frac{K_R C_e}{1 + a_R C_e^{\beta}}$

The process of gas phase adsorption is influenced by both the adsorbate properties and the adsorbents properties. The pore size distribution of the adsorbent strongly affects adsorption [42]. The ACSNB in which large pores predominate has higher capacity than those with predominant small pores [42]. (Fig. **11**) clearly indicates that 2:1 impregnation ratio has higher pore volume compare to that of 1:1 impregnation ratio. This property is in accordance with the experimental data for benzene. In physical adsorption, benzene gas molecules get adhered on to the activated biomass is also dominated by interaction potentials of adsorbate on the adsorbent surface: the van der Waals forces attraction; electro static interactions comprising polarization, dipole moment reported by Kim *et al.* [42]. Gas molecules has strong dipole moment, the adsorption of this gas molecule increases as the field of dipole interaction becomes significant reported by [49]. This property could play a role in the adsorption potential. This may be explained by relationship between the surface of activated carbon and benzene vapors. Benzene molecule has non polar due to C-C bond. Also, because the activated carbon used in this study has non polar and hydrophobicity, the adsorption ability of benzene vapor with non polar nature is higher than that of polar nature reported by Lee *et al.* [43]. This result indicates that activated carbon displays a high affinity toward non-polar organic compounds. K_F and 1/n indicate the adsorption capacity and adsorption intensity, respectively. The higher the value of 1/n, the higher will be the affinity and the heterogeneity of the adsorbent sites. It is found from Table **3** that the ACSNB shows no specific trend of heterogeneity with 303 K. Values of 1/n less than 1 showed favorable nature of adsorption of benzene on ACSNB [60-61]. It is also noted that the R–P constant normally lies between 0 and 1, indicating favorable adsorption. Similar Langmuir equation was fitted for adsorption of Methylene Blue onto Hazelnut Shells [62].

Error Analysis

Four different error functions were employed in this study to find out the most suitable isotherm model to represent the experimental data. These error functions were given in Table **4**. The most commonly used one, the sum of the SSE function, has a major drawback in that it provides isotherm parameters showing a better fit at the higher end of the adsorbate concentration. This is because magnitude of the errors and hence the square of errors increases as the adsorbate concentration increases. The HYBRID was used, in order to improve the fit of the SSE method at low concentration values by dividing by the measured value. In

Table 4. Values of Four Different Error Analyses of Isotherm Models for Adsorption of Benzene by ACSNB (t=120 min, C_0= 300–500 mg/l, m=10 g/l)

		1:1						2:1			
Conc. (mg/l)	**Models**	**MPSD**	**HYBRID**	**SSE**	**CHI2**	**Conc. (mg/l)**	**Models**	**MPSD**	**HYBRID**	**SSE**	**CHI2**
300	**Langmuir**	9.776	6.769	594.90	5.475	**300**	**Langmuir**	30.791	19.352	860.589	16.816
	Freundlich	20.123	17.172	5280.599	37.179		**Freundlich**	27.831	21.317	9734.497	80.852
	Temkin	18.638	14.019	6396.003	39.358		**Temkin**	47.633	38.543	16712.14	148.613
	R-P	7.953	4.727	727.37	6.025		**R-P**	40.637	35.804	7771.305	77.285
400	**Langmuir**	18.679	13.912	6130.997	31.829	**400**	**Langmuir**	39.854	30.701	13429.3	85.812
	Freundlich	14.197	10.712	7160.568	35.080		**Freundlich**	36.643	29.653	15218.99	106.483
	Temkin	29.231	25.866	37400.33	152.364		**Temkin**	43.162	32.555	76848.75	348.062
	R-P	14.495	10.688	5667.106	22.091		**R-P**	39.974	30.915	5942.587	63.487
500	**Langmuir**	18.204	13.074	7594.154	34.847	**500**	**Langmuir**	27.008	17.791	8652.03	55.827
	Freundlich	35.232	18.072	8157.529	46.604		**Freundlich**	36.881	19.008	3587.184	42.392
	Temkin	36.742	29.670	133257.7	386.346		**Temkin**	38.747	28.417	149468.1	437.496
	R-P	18.470	13.299	7695.364	35.696		**R-P**	26.049	16.926	2162.75	26.186

$$MPSD = 100\sqrt{\frac{1}{n_m - n_p}\sum_{i=1}^{n}\left(\frac{q_{e,i,\exp} - q_{e,i,cal}}{q_{e,i,\exp}}\right)^2} \; ; \; HYBRID = \frac{100}{n-p}\sum_{i=1}^{n}\left[\frac{(q_{e,\exp} - q_{e,calc})}{q_{e,\exp}}\right]_i ;$$

$$SSE = \sum_{i=1}^{n}(q_{e,\exp} - q_{e,cal})_i^2 \; ; CH = \sum_{i=1}^{n}\left[\frac{(q_{e,\exp} - q_{e,calc})}{q_{e,\exp}}\right]_i$$

addition a divisor was included as a term for the number of degrees of freedom for the system—the number of data points (n) minus the number of parameters (p) within the isotherm equation. MPSD error function similar in some respects to a geometric mean error distribution modified according to the number of degrees of freedom of the system and sum of the absolute errors (CH). The values of the error functions are presented in Table **4**. The fit of various isotherm models tested for the adsorption of benzene onto ACSNB at 303K is compared in (Figs. **10** and **11**). By comparing the results of the error values, it was found that the Langmuir isotherm best fitted benzene adsorption isotherm datas for the ACSNB at 303K.

EFFECT OF INLET CONCENTRATION ON BREAKTHROUGH CURVE OF THE ACNSB COLUMN ABSORBER

The breakthrough characteristics according to inlet concentration of benzene, an adsorption experiment was carried out at room temperature in the following conditions: inlet concentration of adsorbate 200-700 mg/l and adsorbents 1:1 and 2:1 impregnation ratio. The breakthrough curves of benzene according to inlet concentrations are compared as shown in (Figs. **12a & b**). The higher inlet concentration of adsorbate, faster breakthrough and slope of breakthrough curve was gradually increased. The variation range of breakthrough curve of 2:1 impregnation ratio was not larger than that of 1:1 impregnation ratio. In (Figs. **12a & b**) breakthrough time defined as time when outlet concentration was 70% of inlet concentration. For (Figs. **12a** and **b**) as the inlet concentration of benzene was increased from 200-700 mg/l, the breakthrough time got decreased from 480 to 220 min, and for (Figs. **12a** and **b**) inlet concentration of benzene was increased from 200-700 mg/l, the breakthrough time was decreased from 600 to 360 min. Therefore, as inlet concentrations benzene were increased, the breakthrough time was decreased, but the equilibrium adsorption capacities of benzene were increased. This result is explained by the fact that allowable adsorbate molecules are increased as increasing adsorbate concentration and also, the adsorption is fast as much as the increase of diffusion velocity and adsorption velocity into pores of ACSNB, so time to reach equilibrium is reduced. It was thought that the increase of adsorption capacity according to increasing adsorbate concentration was due to the increase of concentration differences that is driving force in mass transfer [43].

Effect of Adsorbents on Breakthrough Curve

From (Figs. **13 a, b & c**) shows breakthrough curves of benzene under different concentrations onto ACSNB (1:1 and 2:1 impregnation ratio). The concentration of effluent increased gradually with time at all inlet concentrations, suggesting a larger mass transfer resistance, 2:1 impregnation ratio have narrow pore entrance leading to a adsorption rate. Hence, a long time was required to reach equilibrium [48]. It was obvious that the breakthrough times decreased with increasing inlet concentration for all samples.

Moreover, the breakthrough curves became steep with increasing inlet concentrations. For a given concentration, the longer breakthrough time indicated a greater adsorption capacity. (Figs. **13**), the higher the specific surface area, the longer the breakthrough time. However, due to considerable surface complexes on the adsorbent surface, leading to an enhancement of adsorption for non polar adsorbate, benzene adsorption capacity for 1:1 impregnation ratio was lower than 2:1 impregnation ratio, resulting in shorter breakthrough time of benzene explained by [48].

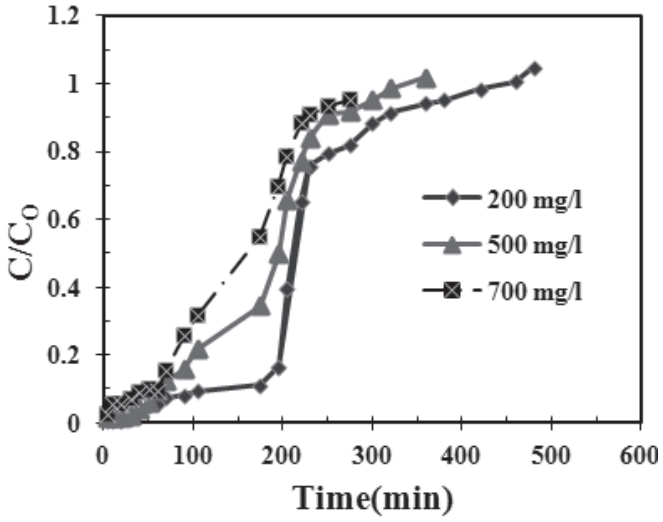

(a)

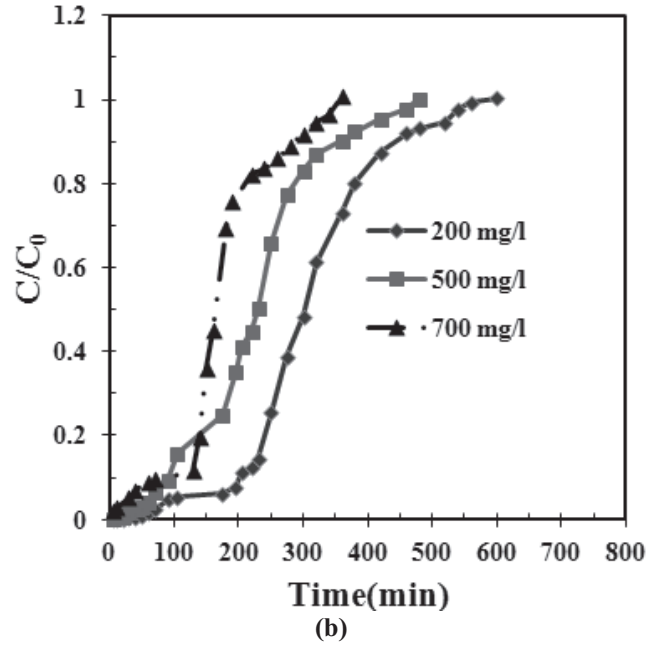

(b)

Fig. (12). Effect of inlet concentration of benzene adsorption in an ACNSB column at 303 K with different concentration; (**a**) 1:1 (**b**) 2:1 impregnation ratio.

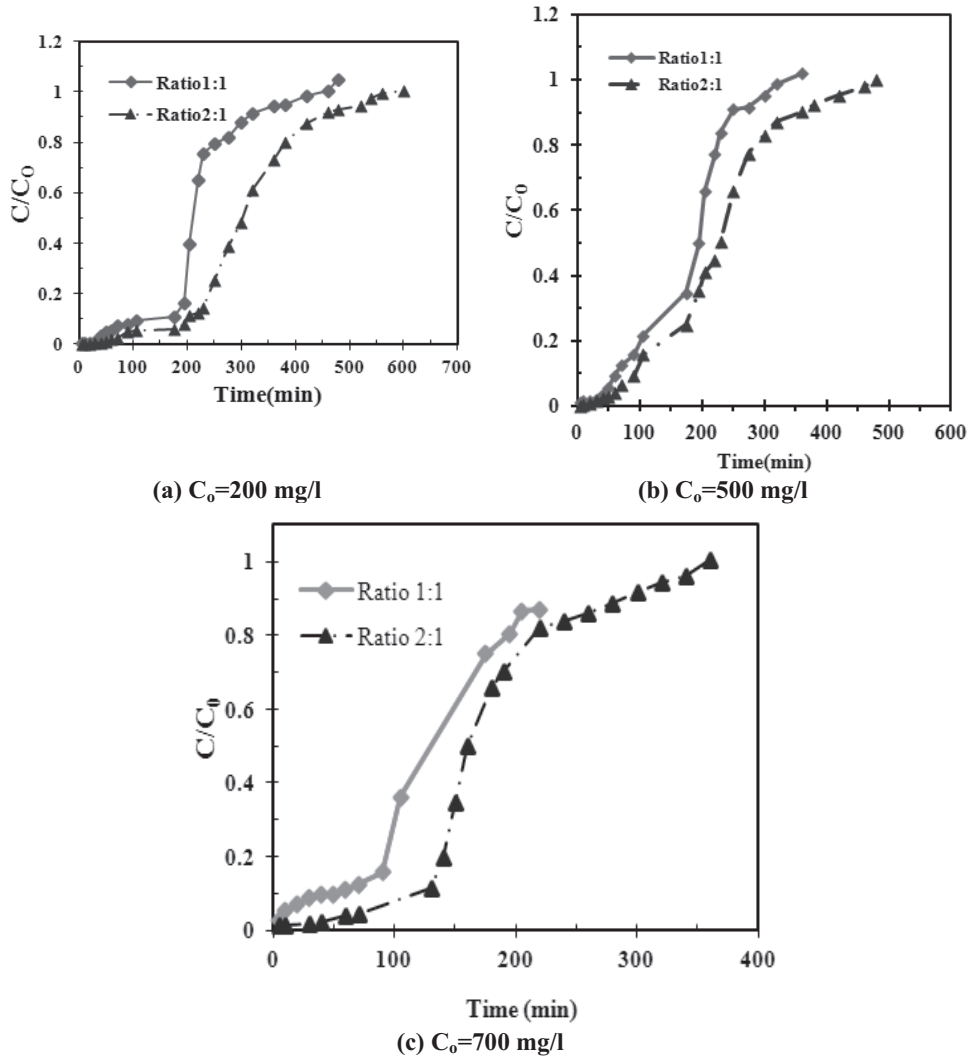

Fig. (13). Effect of ACNSB (1:1 and 2:1 impregnation ratio) on benzene adsorption in an activated CNSB column at 303 K; (**a**) 200 mg/l (**b**) 500 mg/l (**c**) 700 mg/l.

CONCLUSIONS

ACSNB has been used as the most versatile adsorbent for effective removal of benzene vapor. SEM analysis, 2:1 impregnation ratio adsorbent has higher pore development, pore volume and carbon content. Most of pores are cylindrical pores having circular shape while compared to 1:1 impregnation ratio adsorbent. Different types of pores that are spherical shape, slit-shaped pores, and cylindrical pores were observed. The pore development and pore volume is function of activating agent. After adsorption of benzene, change in colour and formation of cavities was higher in case of 2:1 impregnation ratio, because the rate of adsorption is function of pore development and pore volume. Particles size was estimated in the range of approximately 25nm by TEM technique. FT-IR analysis, some basic amine functional groups are formed on the surface of adsorbents (1:1 and 2:1), quite similar for both adsorbents. In a constant volume batch studies for 1:1 and 2:1 impregnation ratio, it can be concluded that, percent removal of benzene increased with increased in time and mass of adsorbents. A higher percentage of benzene removal by ACSNB was possible provided that the C_0 was low. The sorption capacity 2:1 impregnation ratio is 2 times higher than 1:1 impregnation ratio. The optimum adsorbent dose was m =10 g/l of solution. The equilibrium between the adsorbate in the solution and on the adsorbent surface was practically achieved at 120 min. Adsorption kinetics was followed a second-order rate expression. Equilibrium adsorption data for benzene on ACSNB were best fitted by Langmuir isotherm followed by Redlich–Peterson isotherm. In ACNSB column experiments, it can be concluded when inlet concentration of benzene increases with breakthrough time was faster due to higher the pores on the adsorbent (2:1 impregnation ratio), and hence higher adsorption capacity.

CONFLICT OF INTEREST

The author declares no conflict of interest.

ACKNOWLEDGEMENT

Our thanks to NITK and MANITB for providing necessary facilities and to ministry of Human Resource Development, Government of India for financial support.

REFERENCES

[1] EC (European Commission), Environment Fact Sheet: Moving towards clear air for Europe, August 2005, European Commission. (http://ec.europa.eu/environment/pubs/pdf/factsheets/air.pdf, accessed on 5th November 2009). Council Directive 1999/13/EC on the limitation of emissions of VOCs due to the use of organic solvents in certain activities and installations is part of the overall strategy to reduce pollution, 2006.

[2] Kirubakaran CJ, Krishnaiah K, Seshadri SK. Experimental study of the production of activated carbon from coconut shells in a fluidized bed reactor. Ind Eng Chem Res 1991; 30: 2411-2416.

[3] Mohan D, Singh KP. Single- and multi-component adsorption of cadmium and zinc using activated carbon derived from bagasse—an agricultural waste. Water Res 2002; 36: 2304-2318.

[4] Namasivayam C, Sangeetha D. Equilibrium and kinetic studies of adsorption of phosphate onto $ZnCl_2$ activated coir pith carbon. J Colloid Interface Sci 2004; 280: 359-365.

[5] Sahu JN, Agarwal S, Meikap BC, Biswas MN. Performance of a modified multi-stage bubble column reactor for lead(II) and biological oxygen demand removal from wastewater using activated rice husk. J Hazard Mater 2009; 161: 317-324.

[6] Ricordel S, Taha S, Cisse I, Dorange G. Heavy metals removal by adsorption onto peanut husks carbon: characterization, kinetic study and modelling. Sep Purif Technol 2001; 24: 389-401.

[7] Mohanty K, Jha M, Meikap BC, Biswas MN. Removal of chromium (VI) from dilute aqueous solutions by activated carbon developed from Terminalia arjuna nuts activated with zinc chloride. Chem Eng Sci 2005; 60: 3049-3059.

[8] Singh CK, Sahu JN, Mahalik KK, Mohanty CR**,** Raj Mohan B, Meikap BC. Studies on the removal of Pb(II) from wastewater by activated carbon developed from Tamarind wood activated with sulphuric acid. J Hazard Mater 2008; 153: 221-228.

[9] Ali I, Gupta VK, Advances in Water Treatment by Adsorption Technology, Nature Protocols, 2006; 1: 2661-2667.

[10] Gupta VK, Carrott PJM, Carrott MMLR, Suhas, Low-Cost adsorbents: Growing approach to wastewater treatment a review Crit Review Environ Sci Technol 2009a; 39: 783-842.

[11] Gupta VK, Mittal A, Jain R, Mathur M, Sikarwar S, Adsorption of Safranin-T from wastewater using waste materials- activated carbon and activated rice husks. J Colloid Interf Sci 2006a; 303: 80-86.

[12] Gupta VK, Ali I, Removal of Endosulfan and Methoxychlor from Water on Carbon Slurry. Environ Sci Technol 2008; 42:766-770.

[13] Gupta VK, Ali I, Saini VK, Adsorption studies on the removal of Vertigo Blue 49 and Orange DNA13 from aqueous solutions using carbon slurry developed from a waste material. J Colloid Interf Sci 2007a; 315: 87-93.

[14] Gupta VK, Jain R, Varshney S, Removal of Reactofix golden yellow 3 RFN from aqueous solution using wheat husk--An agricultural waste., J Hazard Mater 2007b; 142: 443-448.

[15] Gupta VK, Mittal A, Gajbe V, Mittal J. Removal and Recovery of the Hazardous Azo Dye Acid Orange 7 through Adsorption over Waste Materials: Bottom Ash and De-Oiled Soya. Ind Eng Chem Res 2006b; 45: 1446-1453.

[16] Girgis BS, El-Hendawy AA. Porosity development in activated carbons obtained from date pits under chemical activation with phosphoric acid. Microspores Mesopores Material 2002; 52: 105-117.

[17] Kang SW, Min BH, Suh SS. Breakthrough behavior of benzene and toluene in adsorption bed. J Kor Oil Chem Soc 2000; 17: 83.

[18] Kim SJ, Cho SY, Kim TY. Adsorption of chlorinated volatile organic compounds in a fixed bed of activated carbon. Korean J Chem Eng 2002 19: 61.

[19] Puri BR. In: Walker, P.L. (Ed.), Chemistry and Physics of Carbon. Marcel Dekker, New York, 1970; 191.

[20] Zhang WJ, Rabiei S, Bagreev A, Zhuang MS, Rasouli F. Study of NO adsorption on activated carbons. Appl. Catalysis B: Environ 2008; 83: 63-71.

[21] Bhatia S, Abdullah AZ, Wong, CT. Adsorption of butyl acetate in air over silver-loaded Y and ZSM-5 zeolites: Experimental and modelling studies. J Hazard Mater 2009; 85:73-81.

[22] Popescu M, Joly JP, Carre J, Danatoiu C. Dynamical adsorption and temperature-programmed desorption of VOCs (toluene, butyl acetate and butanol) on activated carbons. Carbon 2003; 41: 739.

[23] Harikrishnan R, Srinivasan MP, Ching CB. Adsorption of ethyl benzene on activated carbon from supercritical CO_2. AIChE J 1998; 44: 2620-2627.

[24] Kim DJ, Shim WG, Moon H. Adsorption equilibrium of solvent vapors on activated carbons. Korean J Chem Eng 2001b; 18: 518.

[25] Kim HS, Park YS, Min BM. Adsorption characteristics of benzene at the fixed-bed adsorption column. J Kor Soc Environ Engrs 2001a; 23: 1979.

[26] Yun JH, Choi DK, Kim SH, Moon H. Effects of non-ideal adsorption equilibria of gas mixtures on column dynamics. Korean J Chem Eng 1997; 14: 369.

[27] Ingle TR, Vaidya SH, Pai MU. Improvements in or related to manufacture of cashew nut shell gum (CNS-Gum). Indian Patent No 123638 (1971).

[28] Ingle TR, Vaidya SH, Pai MU. Process for preparation of D-Galactose from Cashew nut shells, Indian patent No 137999, 1976.

[29] Tyman JHP, Patel MS, Manzara AP.Treatment of cashew nut shell liquid. U.S. Patent 4,352,944, 1982.

[30] Mondal PK, Dohhen KC, Sarin R, Tuli DK, Raje NR, Bhatnagar AK. Process for preparing rust inhibitors from cashew nut shell liquid, US patent. 6548459, 2003.

[31] Roux, Sathe KH, Shridhar K, Teuber, Suzanne S. Purified linear epitopes from cashew nuts, nucleic acids encoding therefor, and associated methods, Patent 7381534 Issued on June 3, 2008.

[32] Roux K, Teuber, Suzanne S, Shridhar K, Robotham J. Nucleic acid and allergenic polypeptides encoded thereby in cashew nuts, Patent 7763709 Issued on July 27, 2010.

[33] Nagashima, KSC, Mochizuki MSC. Composition for a feed and a feed each containing cashew nut shell liquid (CNSL) and/or anacardic acids and an oil sorbent European Patent WO 2009/151048, EP 2 298 082 A1, 2011.

[34] Kittredge JB, Lake Minn. WB, Micchelli, St. Paul Minn NJ, Phenolic Polyamino-amides capable of curing epoxy resins, US patent 3382261, 1968.

[35] Bussell GW. Maleinized fatty acid esters of 9-oxatetracyclo-4.4.1.-O,O-undecan-4-ol. US Patent 3,855,163; 1974.

[36] Hodakowski LE, Osborn CL, Harris EB. Polymerizable epoxide modified compositions. US Patent 4,119,640; 1978.

[37] Gratuito MKB, Panyathanmaporn T, Chumnanklang R-A, Sirinuntawittaya N, Dutta A. Production of activated carbon from coconut shell: Optimization using response surface methodology. Bioresour Technol 2008; 99: 4887-4895.

[38] Brunauer S, Emmet PH, Teller F. Adsorption of Gases in Multimolecular Layer. J Am Chem Soc 1938; 60: 309.

[39] Astm D 4607-94, Standard Test Method for Determination of Iodine Number of Activated Carbon', ASTM Committee on Standards, ASTM D 4607-94; ASTM: Philadelphia, PA, USA, 2006.

[40] Sene L, Converti A, Felipe MGA, Zilli M. Sugarcane bagasse as alternative packing material for biofiltration of benzene polluted gaseous streams a preliminary study. Bioresour Technol 2002; 83: 153-157.

[41] Lodge JP. Methods of Air sampling and analysis. Lewis Publishing Inc, New York, NY, 1989.

[42] Kim D, Cai Z, Sorial GA. Determination of gas phase adsorption isotherms a simple constant volume method. Chemosphere 2006; 64: 1362-1368.

[43] Lee M-G, Lee S-W, Lee S-H. Comparison of vapor adsorption characteristics of acetone and toluene based on polarity in activated carbon fixed-bed reactor. Korean J Chem Eng 2006; 23: 773-778.

[44] Choi D-Y, Lee J-W, Jang S-C, Ahn B-S, Choi D-K. Adsorption dynamics of hydrogen sulfide in impregnated activated carbon bed. Adsorption 2008; 14: 533-538.

[45] Tansel B, Nagarajan P. SEM study of phenolphthalein adsorption on granular activated carbon. Advances Environ Res 2004;8: 411-415.

[46] Guo J, Lua AC. Effect of surface chemistry on gas-phase adsorption by activated carbon prepared from oil-palm stone with pre-impregnation. Sep Puri Technol 2000; 18: 47-55.

[47] Suresh S, Srivastava VC, Mishra IM. Study of catechol and resorcinol adsorption mechanism through granular activated carbon characterization, pH and kinetic study. Sep Sci. Technol., 2011b; 46: 1750 -1766.

[48] Huang Z-H, Kang F, Liang K-M, Hao J. Breakthrough of methyethylketone and benzene vapors in activated carbon fiber beds. J Hazard Mater 2003; B98: 107-115.

[49] Yang RT. Adsorbents: Fundamentals and Applications. John Wiley & Son, Inc., Hoboken, NJ, 2003.

[50] Lagergren S. About the theory of so-called adsorption of soluble substances. Kungliga Svenska Vetenskapsakademiens Handlingar 1898; 24: 1-6.

[51] Ho YS, McKay G. 1999. Pseudo-second-order model for sorption processes. Process Biochem 1999; 34: 451-465.

[52] Marquardt DW. An algorithm for least-squares estimation of nonlinear parameters. J Soc Appl Mathematics 1963; 11:431-441.

[53] Porter JF, McKay G, Choy KH. The prediction of sorption from a binary mixture of acidic dyes using single- and mixed isotherm variants of the ideal adsorbed solute theory. Chem Eng Sci 1999; 54: 5863-5885.

[54] Ng JCY, Cheung WH, McKay G. Equilibrium studies for the sorption of lead from effluents using chitosan. Chemosphere 2003; 52: 1021-1030.

[55] Weber Jr, WJ, Morris JC. Kinetics of adsorption on carbon from solution. J Sanitary Eng Division-ASCE 1963; 89: 31-59.

[56] Freundlich HM F. Over the adsorption in solution. J Phys Chem 1906; 57: 385-471.

[57] Langmuir I. The adsorption of gases on plane surfaces of glass, mica and platinum. J Am Chem Soc 1918; 40: 1361-1403.

[58] Redlich O, Peterson DL. A useful adsorption isotherm. J Phys Chem 1959; 63: 1024-1026.

[59] Temkin MI, Pyzhev V. Kinetics of ammonia synthesis on promoted iron catalysts. Acta Physiochimica URSS 1940; 12: 327-356.

[60] Faust SD, Aly OM. Adsorption Processes for Water Treatment. Butterworths, London, 1987.

[61] Suresh S, Srivastava, VC, Mishra IM. Isotherm, thermodynamics, desorption and disposal study for the adsorption of catechol and resorcinol onto granular activated carbon. J Chem Eng Data 2011a; 56: 811-818.

[62] Dogan M, Abak H, Alkan M. Biosorption of Methylene Blue from Aqueous Solutions by Hazelnut Shells: Equilibrium, Parameters and Isotherms. Water Air Soil Pollut 2008; 192: 141-153.